ON THE OPTIMAL PLACEMENT OF PZT ACTUATORS FOR THE CONTROL OF THE DYNAMIC RESPONSE OF A BEAM

Renato BARBONI, Enrico FANTINI, Paolo GAUDENZI, Alessandro MANNINI
Universita' di Roma "La Sapienza", Dipartimento Aerospaziale
Via Eudossiana 16, 00184 Roma, Italy

Abstract

Aim of this work is to find the dynamic influence functions of an Euler-Bernoulli beam under different boundary conditions actuated by a couple of PZT patches and to investigate about their use in the dynamics of an active beam. A modal approach is used to build the dynamic influence functions in such a way that not only the position of the PZT actuators but also their size can be directly taken into account. Several analysis concerning the controllability of the dynamic response of the beam and in particular the possibility of exciting some desired modes are presented. Finally simple optimization problems concerning the placement and the size of the actuator are solved.

Nomenclature

b_b	beam width
b_a	actuator width
d_{31}	piezoelectric strain coefficient
E_b	Young's modulus of the beam
E_a	Young's modulus of the actuator
t_b	beam thickness
t_a	thickness of the actuator
h	length of the actuator
a	position of the center of PZT
V	voltage applied to the actuator
w	deflection of the beam
M_a	equivalent bending moment
Λ	free strain of the actuator
μ	mass per unit length of the beam
ω_i	i-th natural frequency of the beam
X_i	i-th eigenmode of the beam
Φ_i	i-th modal amplitude
Ω	dimensionless loading frequency
I_a	moment of inertia of the actuator
I_b	moment of inertia of the beam

1 Introduction

In the last years there has been a large number of studies on the possible use of distributed actuators and sensors in the frame of the 'intelligent', or 'smart' materials technology, which makes focus on the possibility to build biologically-inspired structures capable of changing their shape, self-detecting and self-repairing internal damages, adapting to different environmental conditions [1],[2] .

Among the various available materials for smart structures actuators and sensors, lead zirconate titanate piezoceramic materials (PZT [3]) are very attractive [4]: they can undergo mechanical strain when subjected to an applied electric field and generate an electric field in response to mechanical stresses and strains. They are easy to be bonded to the structure, and their high stiffness makes possible to induce high strain energy in the system.

In fact it is possible to bond or even embedd these materials to a passive traditional structure [4] to perform both sensing and actuation functions, provided that appropriate placement and size is chosen for them.

A number of models have been proposed to represent the static and dynamic interaction between the PZT and the structures, like the static Pin-Force model by Crawley and de Louis [4] [5] [6] [7] that can be used for active beams, the two-dimensional model for plates developed by Fuller and Rogers [8] and a number of finite-elements approaches [9],[10],[11].

A large number of studies have been also done in the active and passive vibration control of uniaxial structures [12], [13],[14], plates [10], [15],[16], [17] and cylinders [18], also using self-sensing PZT actuators [19],[20].

In this work a modal approach will be used to perform the dynamic influence functions of an undamped Euler-Bernoulli beam, activated in bending by a couple of PZT patches driven out of phase armonically; the static Pin-Force model is here used in the case of dynamic actions.

Since the major interest is here directed to obtain the best geometric conditions that allow a good employement of the PZT as actuators as well as sensors, the presence of internal damping is neglected. In fact in such a case the presence of damping does not change significantly the nature of the problem.

On the contrary very significant changes in the dynamic response of the system depend upon the position and the dimensions of the PZT actuators [21], [15], so an accurate analysis of such a relationship

is performed. The advantage of using the influence functions is that an analytical approach can be used to determine the optimal design variables such as the length and the location of the PZT patch.

2 The actuator/beam interaction

An Euler-Bernoulli beam actuated by two PZT patches bonded respectively on the top and the bottom of the beam , driven out of phase by an electrical field is considered.
We assume that (Pin Force Model [4]): the actuators are perfectly bonded to the structure, their mass is negligeable with respect to the mass of the beam, the presence of the thickness of the actuators do not affect significantly the bending stiffness of the beam.
The dynamic as well as the static actuation of the PZT on the beam can be considered equivalent to two concentrated moments with opposite signs acting at the edges of the couple of piezoelectric patches [4], as shown in figure 1, where:

$$M_a = \frac{\Psi}{6+\Psi} E_a b_a t_a t_b \Lambda \tag{1}$$

and

$$\Lambda = d_{31}\frac{V}{t_a} \qquad \Psi = \frac{E_b I_b}{E_a I_a} \tag{2}$$

d_{31} is the piezoelectric strain coefficient between the applied voltage in the z direction and the resulting free actuation strain Λ along the axis x of the beam.

3 The Dynamic Influence Functions

The deflection $w(x,t)$ of the beam is expanded into the series:

$$w(x,t) = \sum_{i=1}^{\infty} \Phi_i(t) X_i(x) \tag{3}$$

where $X_i(x)$ is the i-th eigenmode of the beam, and $\Phi_i(t)$ the corresponding modal coordinate. We take the virtual displacement

$$\delta w_i = \delta\Phi_i X_i \tag{4}$$

for the i-th mode.
The derivatives with respect to the space coordinate x and the time t will be denoted by primes and dots:

$$\frac{\partial(...)}{\partial x} = (...)' \qquad \frac{\partial(...)}{\partial t} = \dot{(...)}$$

The virtual work of the elastic forces is expressed as:

$$\delta W_E = -E_b I_b \sum_i \Phi_i \delta\Phi_i \int_0^L (X_i'')^2 dx \tag{5}$$

and the virtual work of the inertial forces is:

$$\delta W_I = -\mu \sum_i \ddot{\Phi}_i \delta\Phi_i \int_0^L X_i^2 dx \tag{6}$$

The virtual work of the concentrated actuation moments, can be expressed as:

$$\delta W_{M_a} = M_a[\delta w'(x_2) - \delta w'(x_1)] =$$

$$= M_a \sum_i \delta\Phi_i [X_i'(x_2) - X_i'(x_1)] \tag{7}$$

where x_1 and x_2 represent the locations of the edges of the PZT.
In this way, by superimposing the effects of two concentrated moments acting on the edges of actuators, the mechanism of the actuation of the PZT patches is directly accounted for in the formulation. As a consequence parameters the length h and the position a of the actuator will appear explicitly in the expressions of the influence functions.
The principle of the virtual works can be written as:

$$\delta W_E + \delta W_I + \delta W_{M_a} = 0 \tag{8}$$

By substituting eqs (5) (6) and (7) into eq. (8) we obtain for the i-th mode:

$$E_b I_b \Phi_i(t) \int_0^L (X_i'')^2 dx + \mu \ddot{\Phi}_i(t) \int_0^L X_i^2 dx =$$

$$= M_a(t)[X_i'(x_2) - X_i'(x_1)] \tag{9}$$

By assuming the following normalized quantities

$$\eta = \frac{x}{L} \qquad \tilde{a} = \frac{a}{L} \qquad \tilde{h} = \frac{h}{L}$$

$$\tilde{t}^2 = t^2 \cdot \frac{E_b I_b}{\mu L^4} \quad \tilde{X}_i = L^{-1} \cdot X_i \quad \tilde{M}_a = \frac{M_a L}{E_b I_b}$$

and

$$\int_0^1 \tilde{X}_i^2 d\eta = 1 \tag{10}$$

it follows that

$$\int_0^1 \left(\frac{\partial^2 \tilde{X}_i}{\partial \eta^2}\right)^2 d\eta = \sigma_i^2 \tag{11}$$

being

$$\sigma_i^2 = \frac{\omega_i^2 \mu}{E_b I_b} L^4 \tag{12}$$

The equation (9) becomes:

$$\frac{\partial^2 \Phi_i}{\partial \tilde{t}^2} + \sigma_i^2 \Phi_i = \tilde{M}_a(\tilde{t}) \frac{\partial \tilde{X}_i}{\partial \eta}\bigg|_{\xi_1}^{\xi_2} \tag{13}$$

where

$$\xi_1 = \tilde{a} - \frac{\tilde{h}}{2} \qquad \xi_2 = \tilde{a} + \frac{\tilde{h}}{2} \tag{14}$$

For sake of simplicity the symbol *tilde* will not be reported in the following expressions.
The solution of the i-th dimensionless differential equation in the case of homogeneous initial conditions reduces to:

$$\Phi_i(t) = \int_0^t M_a(\tau) \frac{\partial X_i}{\partial \eta}\Big|_{\xi_1}^{\xi_2} \frac{\sin \sigma_i(t-\tau)}{\sigma_i} d\tau \qquad (15)$$

As a consequence the deflection of the beam can be expressed as:

$$w(\eta, t, a, h) =$$

$$= \sum_{i=1}^{\infty} X_i(\eta) \frac{\partial X_i}{\partial \eta}\Big|_{\xi_1}^{\xi_2} \int_0^t M_a(\tau) \frac{\sin \sigma_i(t-\tau)}{\sigma_i} d\tau \qquad (16)$$

which represents the dynamic influence function of the deflection of the beam under the action of the couple of PZT patches.
By assuming that the performed actuation moment is:

$$M_a(t) = M_0 \sin \Omega t \qquad (17)$$

it follows that:

$$\int_0^t M_a(\tau) \sin \sigma_i(t-\tau) d\tau =$$

$$= \frac{M_0}{\Omega^2 - \sigma_i^2} (\Omega \sin \sigma_i t - \sigma_i \sin \Omega t) \qquad (18)$$

and

$$w(\eta, t, a, h) =$$

$$\sum_{i=1}^{\infty} X_i(\eta) \frac{\partial X_i}{\partial \eta}\Big|_{\xi_1}^{\xi_2} M_0 \frac{(\Omega \sin \sigma_i t - \sigma_i \sin \Omega t)}{\sigma_i(\Omega^2 - \sigma_i^2)} \qquad (19)$$

The use of the above functions will greatly simplify the search for the optimal length and/or position of a single (couple of) actuator(s) due to the possibility of working with such explicit functions directly in the expressions of the optimal conditions.

4 Applications

In the first set of applications the possibility of exciting the dynamics of the beam according to a single bending mode is examined and the relevant optimal choice for geometric parameters is presented.
In the second set of examples the optimal response of the beam is described in terms of two different objective functions: the mean over a period of the square of deflections or rotations measured at a generic point P^* of the beam and the acoustic energy of the beam.
For the first group of applications it is easy to recognize that the effects of the position and size of the actuator only take place in the term $\frac{\partial X_i}{\partial \eta}\Big|_{\xi_1}^{\xi_2}$. If the length h of the actuator is fixed, in order to find the optimal value of a, it is necessary to impose that:

$$\frac{\partial}{\partial a}\left(\frac{\partial X_i}{\partial \eta}\Big|_{\xi_1}^{\xi_2}\right) = 0 \qquad (20)$$

that leads to the condition:

$$\frac{\partial^2 X_i}{\partial \eta^2}\Big|_{\xi 1} = \frac{\partial^2 X_i}{\partial \eta^2}\Big|_{\xi 2} \qquad (21)$$

This fact means that the actuator must be located on the beam so that its edges correspond to points of equal curvature.
On the other hand when the position a of the actuator is fixed its length h will be found by imposing

$$\frac{\partial}{\partial h}\left(\frac{\partial X_i}{\partial \eta}\Big|_{\xi_1}^{\xi_2}\right) = 0 \qquad (22)$$

that leads to the condition:

$$\frac{\partial^2 X_i}{\partial \eta^2}\Big|_{\xi 1} = -\frac{\partial^2 X_i}{\partial \eta^2}\Big|_{\xi 2} \qquad (23)$$

In such a case the opposites edges of the actuator must be at positions with opposites curvatures. The expressions of the derivatives for different boundary conditions are reported in the Appendix.

To obtain the optimal values of the position a and the length h, both the equations (20) and (22) must be satisfied, and the solution of the problem is found whenever a PZT is placed on the beam so that the curvature in ξ_1 and ξ_2 is zero. In other words this means that to excite a desired mode the actuator must be placed between two consecutive points at which the curvature becomes zero; in this case the center of the PZT lays near a location corresponding to a wave-crest of the mode itself, where the highest strain takes place. On the contrary placing the actuator at a strain node makes the actuation modal force negligeable [4].
In the first example the excitation of the first bending mode is considered for a cantilever beam. In fig.2 the amplitude of the mode as a function of the location a and the length h of the actuator is illustrated. Of course for a fixed value of h the range of a is restricted. The same is true for h if a is fixed. The amplitude of the modal response increases both with the increase of a and the increase of h. There is just one point of maximum corresponding to $\frac{h}{L} = 1$ and $\frac{a}{L} = 0.5$.
Figures 4 and 5 are relevant to the second bending mode. In this case the maximum amplitude is obtained for $\frac{h}{L} = 0.785$ and $\frac{a}{L} = 0.6075$.
For the third mode (fig.6-7) the optimal values are $a = 0.7163$, $h = 0.5025$. In the case of fixed length of the actuator ($h = 0.2$) the optimal solution can

respect only the condition of eq.(20); in fact the position of the actuator is such that the opposite edges have the same curvature (fig.8). In fig.9 the case of fixed position ($a = 0.4$) is illustrated. The solution here satisfies eq. (22) only, that is the condition of opposite curvatures at the edges of actuators. The sixth mode is considered in fig.10 and 11.
In the next diagrams beams with different boundary conditions are examined. Fig.12-13 concern the case of the first mode of a simply-supported/clamped beam, for which the best position of the actuator is the one closer to the simple support. Fig.14-15 and 16-17 illustrate respectively the case of the second mode of a clamped/clamped beam and of the third mode of a simply-supported beam.

For the second group of applications, in the first case the function to minimize is expressed as follows

$$\bar{w}(\eta^*, a, h) = \sqrt{\frac{1}{T}\int_0^T \left(w(\eta^*, t, a, h)\right)^2 dt} =$$

$$= \sqrt{\sum_{i=1}^{N} \bar{\bar{w}}_i^2 + \sum_{i=1}^{N}\sum_{j=i+1}^{N}\left(\int_0^{2\pi} \frac{1}{\pi}\Phi_i\Phi_j dt\right) X_i X_j} \quad (24)$$

where

$$\bar{\bar{w}}_i^2 = \frac{1}{2\pi}\int_0^{2\pi} w_i^2 dt \quad (25)$$

Substituting the expression of eq.(21) and integrating we obtain:

$$\bar{w}(\eta^*, a, h) = \sqrt{\frac{1}{\pi}\sum_{i=1}^{N}\left[A_i + \sum_{j=i}^{N} B_{ij}\right]} \quad (26)$$

with

$$A_i = \left(\frac{M_0 X_i(\eta^*)}{\sigma_i(\Omega^2 - \sigma_i^2)}\frac{\partial X_i}{\partial \eta}\Big|_{\xi_1}^{\xi_2}\right)^2 \cdot$$

$$\left[\pi\left(\Omega^2 + \sigma_i^2\right) - \frac{\Omega^2}{4\sigma_i}\sin 4\pi\sigma_i - \frac{\sigma_i^2}{4\Omega}\sin 4\pi\Omega + \right.$$

$$\left. + \sigma_i\Omega\left(\frac{\sin 2\pi(\sigma_i + \Omega)}{2(\sigma_i + \Omega)} - \frac{\sin 2\pi(\sigma_i - \Omega)}{2(\sigma_i - \Omega)}\right)\right] \quad (27)$$

$$B_{ij} = \frac{M_0^2 X_i(\eta^*) X_j(\eta^*)}{(\Omega^2 - \sigma_i^2)\sigma_i\sigma_j(\Omega^2 - \sigma_j^2)} \cdot \frac{\partial X_i}{\partial \eta}\Big|_{\xi_1}^{\xi_2}\frac{\partial X_j}{\partial \eta}\Big|_{\xi_1}^{\xi_2} \cdot$$

$$\cdot\left[\sigma_i\sigma_j\left(\pi - \frac{\sin 4\pi\sigma_i}{4\sigma_i} - \frac{\sin 4\pi\sigma_j}{4\sigma_j}\right) + \right.$$

$$+\Omega^2\left(\frac{\sin 2\pi(\sigma_i - \sigma_j)}{2(\sigma_i - \sigma_j)} - \frac{\sin 2\pi(\sigma_i + \sigma_j)}{2(\sigma_i + \sigma_j)}\right) +$$

$$+\Omega\sigma_j\left(\frac{\sin 2\pi(\Omega - \sigma_j)}{2(\Omega - \sigma_j)} - \frac{\sin 2\pi(\Omega + \sigma_j)}{2(\Omega + \sigma_j)}\right) +$$

$$\left. + \Omega\sigma_i\left(\frac{\sin 2\pi(\sigma_i - \Omega)}{2(\sigma_i - \Omega)} - \frac{\sin 2\pi(\sigma_i + \Omega)}{2(\sigma_i + \Omega)}\right)\right] \quad (28)$$

In the second case the objective function can be defined as follows:

$$\bar{E} = \sqrt{\frac{1}{T}\int_0^T \int_0^1 \left[w(\eta, t, a, h)\right]^2 d\eta dt} \quad (29)$$

that is the mean-square acoustic energy of the beam. Eq.(29) can be expressed in the following form:

$$\bar{E} = \sqrt{\frac{1}{T}\int_0^T \int_0^1 \left(\sum_{i=1}^{N} w_i\right)^2 d\eta dt} =$$

$$= \sqrt{\frac{1}{T}\int_0^T \int_0^1 \sum_{i=1}^{N}\left(w_i^2 + 2\sum_{j=i+1}^{N} w_i w_j\right) d\eta dt} \quad (30)$$

Being the modes orthonormal we can write:

$$\bar{E} = \sqrt{\sum_{i=1}^{N}\frac{1}{T}\int_0^T \int_0^1 w_i^2 d\eta dt} = \sqrt{\sum_{i=1}^{N}\bar{E}_i^2} \quad (31)$$

with

$$\bar{E}_i^2 = \frac{M_0^2}{\pi\sigma_i^2(\Omega^2 - \sigma_i^2)^2}\left(\frac{\partial X_i}{\partial \eta}\Big|_{\xi_1}^{\xi_2}\right)^2 \cdot$$

$$\cdot\left[(\Omega^2 + \sigma_i^2)\pi - \frac{\Omega^2}{4\sigma_i}\sin 4\pi\sigma_i - \frac{\sigma_i^2}{4\Omega}\sin 4\pi\Omega + \right.$$

$$\left. + 2\sigma_i\Omega\left(\frac{\sin 2\pi(\sigma_i + \Omega)}{2(\sigma_i + \Omega)} - \frac{\sin 2\pi(\sigma_i - \Omega)}{2(\sigma_i - \Omega)}\right)\right] \quad (32)$$

In fig.18 the first objective function is shown as a function of a and h for a bending case of a cantilever beam with $M(t) = \sin\Omega t$. In the numerical process the first seven modes are considered. At a loading frequency close to the first one the first mode is expecially excited, as expected. At fixed values of h the maximum deflection is obtained for the lowest value of a, that is for locations close to the clamped edge. In fig.19 and 20 the values of mean square tip deflection and rotation can be compared for a value of a loading frequency between the first and the second eigenfrequency. It is worth noting that the maximum rotation iis not obtained for the values of h and a for which the maximum displacements is reached. In fig.21 the best exciting conditions for the second mode can be seen: the positions around 0.22 should be avoided if the aim is to excite the second mode. For values of h between 0.4 and 0.5, the best placement to excite the first mode is the worst for exciting

the second mode. Moreover from a comparison between fig.21 and fig.22 respectively relevant to loading frequencies close to the second and third eigenfrequencies, it can be seen that the optimal conditions for the second mode may be the worst for the third mode at least for the lower values of h.
Fig.23-26 show the mean-square acoustic-energy of a cantilever beam built with the first seven terms of the modal expansion. Finally fig.27 shows the optimal geometric conditions for discrete values of the frequencies for a cantilever beam for three significative values of the length h. For small actuators the best placement is close to the clamp if the load frequency is less than the third eigenfrequency, beyond this value the PZT must be placed at about the center of the beam. Larger actuators must be placed near the clamp until the second eigenfrequency is reached.

Acknoledgments

The authors aknoledge the support of CNR contract n^0 95.00034.CT07 (responsible Prof. Barboni). As far as the contribution of the authors to the present paper, on the basis of R.Barboni's idea of using the influence function technique in vibrations problem of active structures, P.Gaudenzi formulated the construction of a special influence function which take directly into account the PZT-patches mechanism of actuation by superposing the effects of two concentrated moments placed at the edges of the actuators. A.Mannini formulated the expressions of the dynamic influence functions and supervised the numerical applications which were studied and run by E. Fantini.

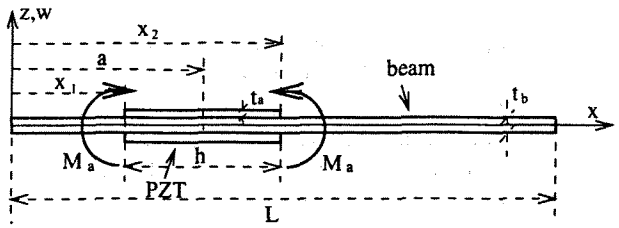

Figure 1: PZT equivalent moment

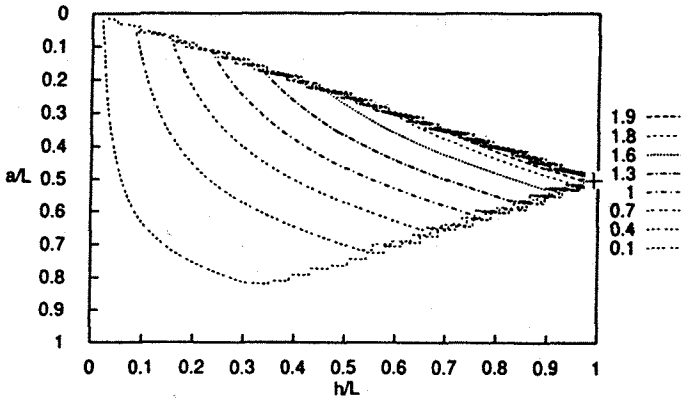

Figure 2: Cantilever beam - amplitude of the first mode as a function of the location and the dimension of the PZT

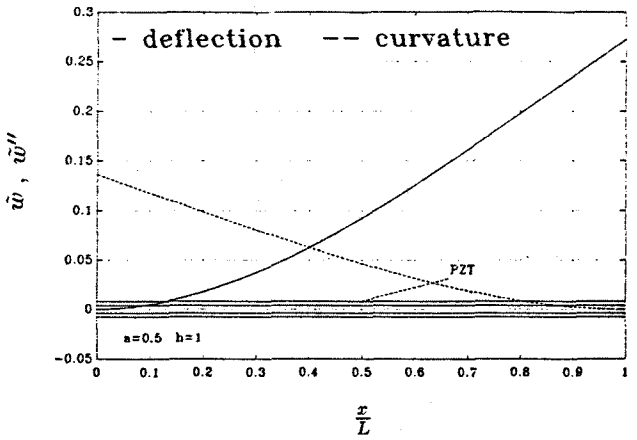

Figure 3: Cantilever beam - Optimal PZT-patch to excite mode 1

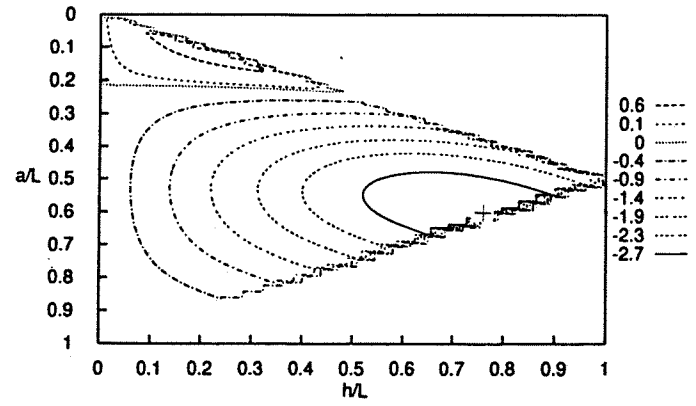

Figure 4: Cantilever beam - amplitude of the second mode as a function of the location and the dimension of the PZT

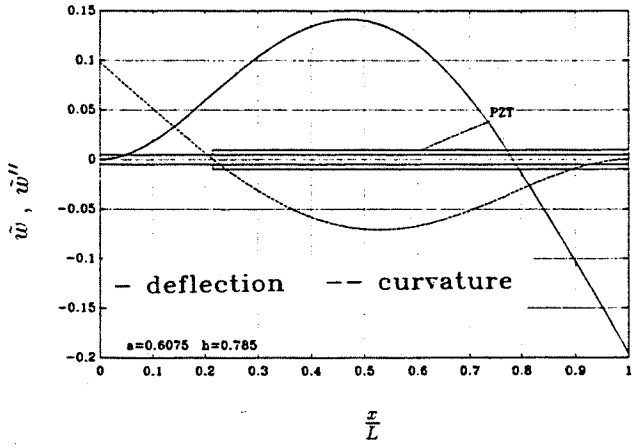

Figure 5: Cantilever beam - Optimal PZT-patch to excite mode 2

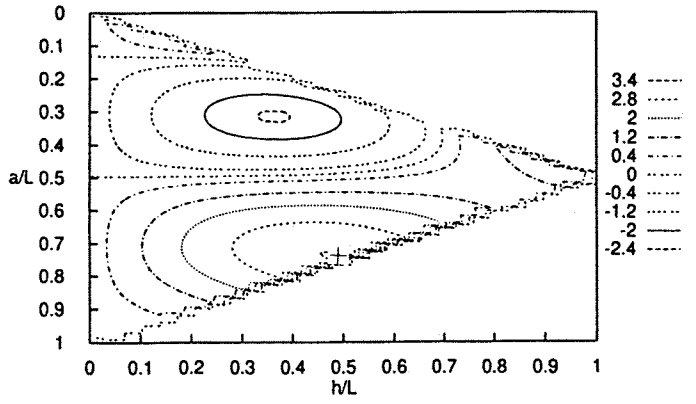

Figure 6: Cantilever beam - amplitude of the third mode as a function of the location and the dimension of the PZT

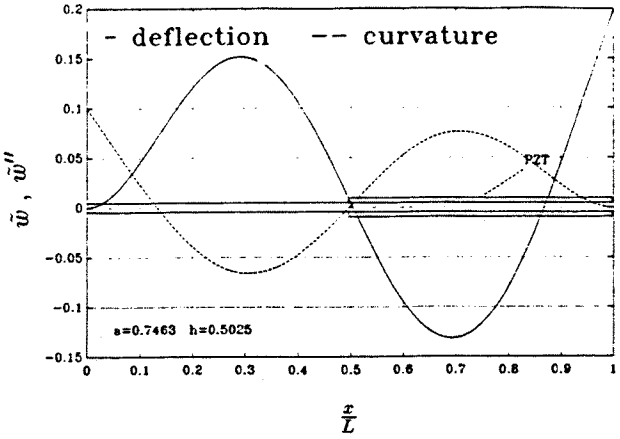

Figure 7: Cantilever beam - Optimal PZT-patch to excite mode 3

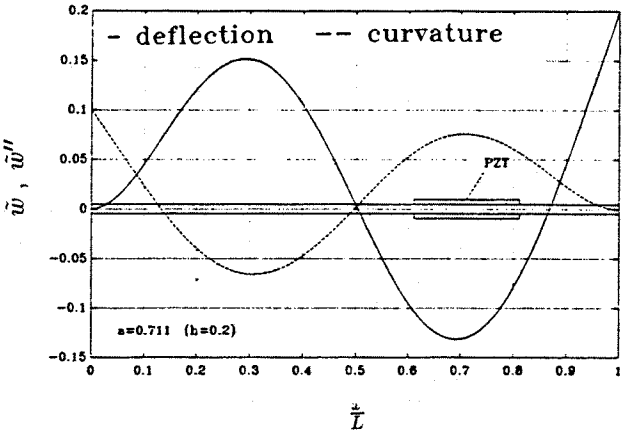

Figure 8: Cantilever beam - Optimal PZT-placement to excite mode 3 (h fixed)

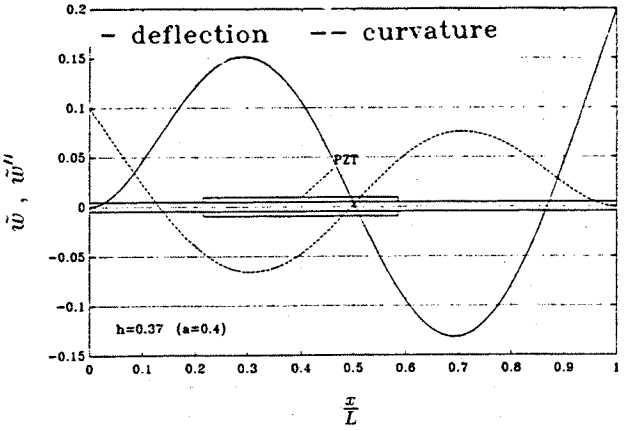

Figure 9: Cantilever beam - Optimal PZT-length to excite mode 3 (a fixed)

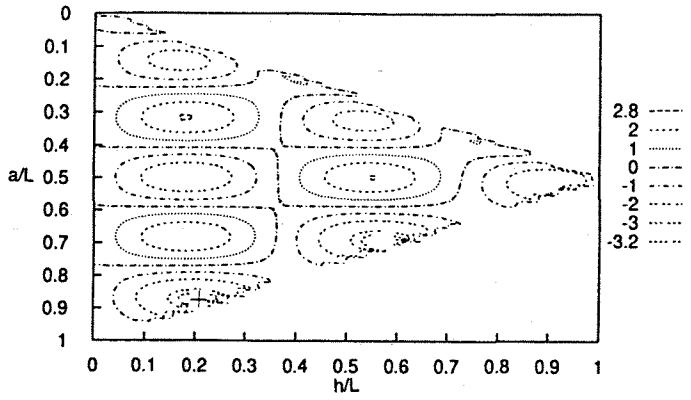

Figure 10: Cantilever beam - amplitude of the sixth mode as a function of the location and the dimension of the PZT

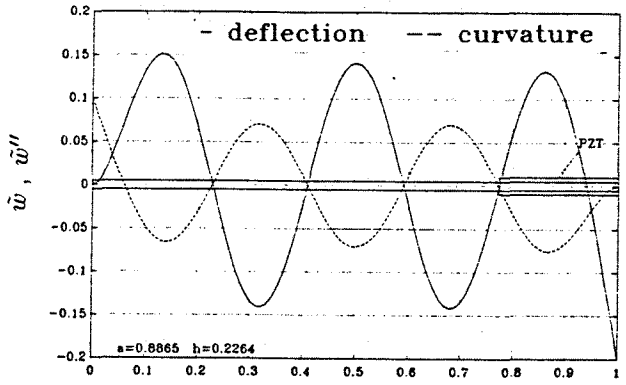

Figure 11: Cantilever beam - Optimal PZT-patch to excite mode 6

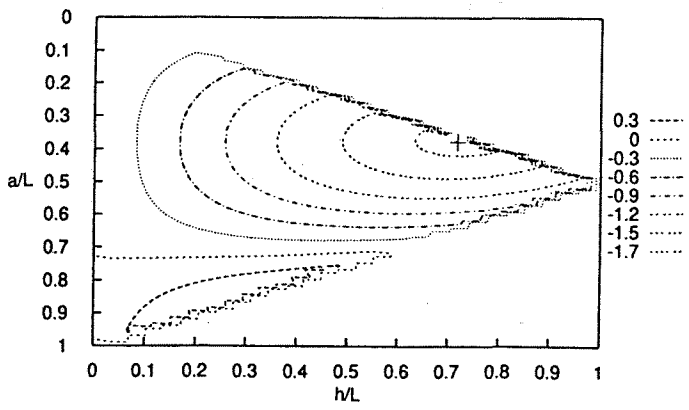

Figure 12: Supported-clamped beam - amplitude of the first mode as a function of the location and the dimension of the PZT

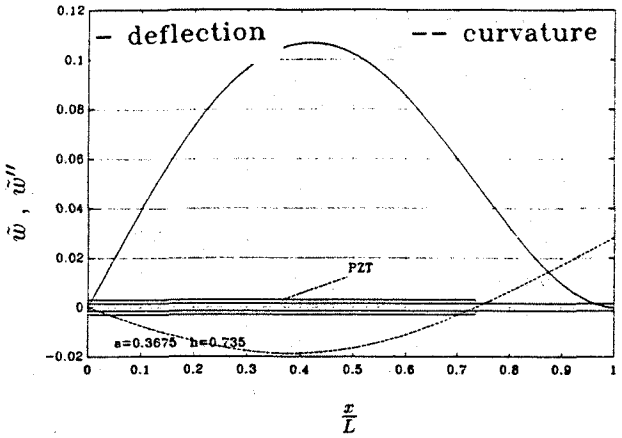

Figure 13: Supported-clamped beam - Optimal PZT-patch to excite mode 1

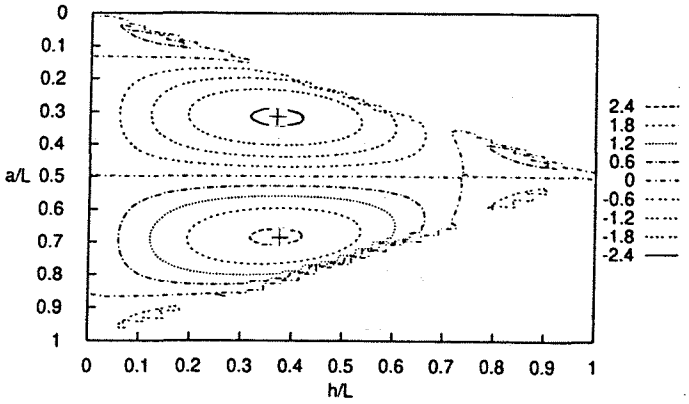

Figure 14: Clamped beam - amplitude of the second mode as a function of the location and the dimension of the PZT

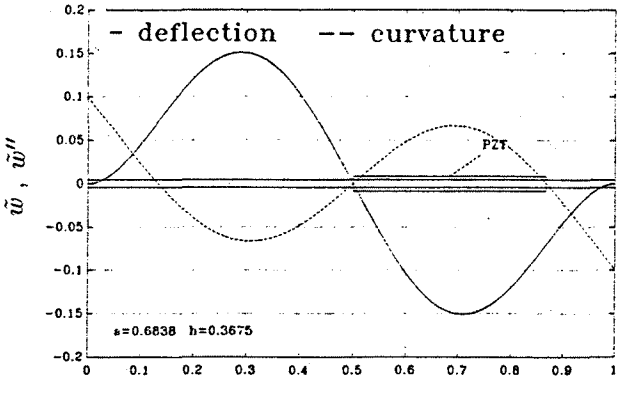

Figure 15: Clamped beam - Optimal PZT-patch to excite mode 2

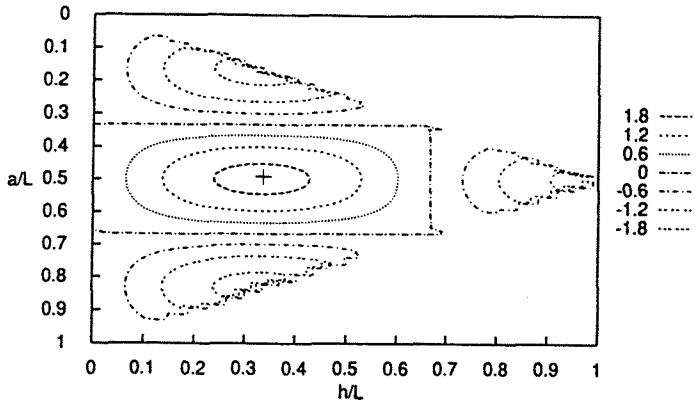

Figure 16: Simply supported beam - amplitude of the third mode as a function of the location and the dimension of the PZT

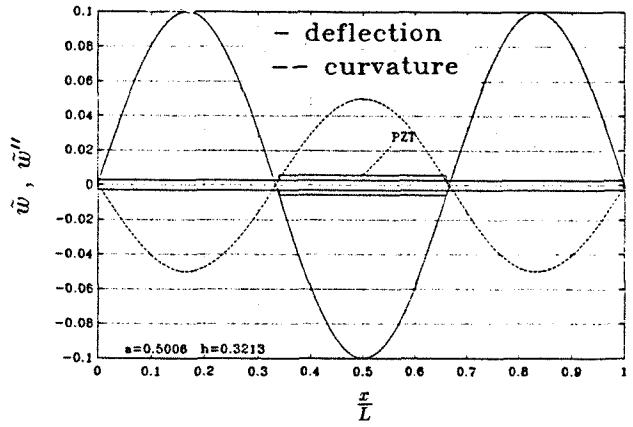

Figure 17: Simply supported beam - Optimal PZT-patch to excite mode 3

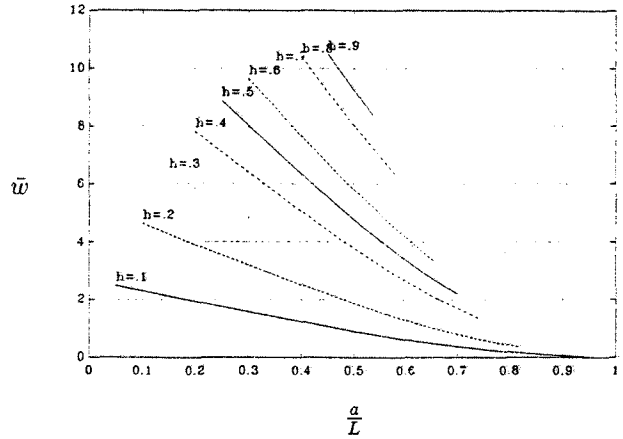

Figure 18: Mean square tip-deflection of a cantilever beam (load frequency = 10.3 rad/s)

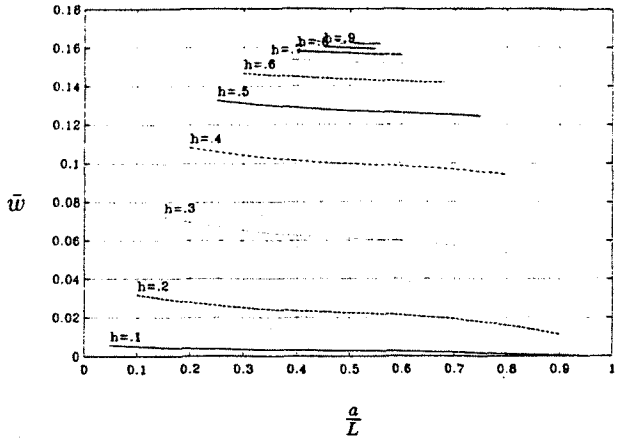

Figure 19: Mean square tip-deflection of a cantilever beam (load frequency = 30 rad/s)

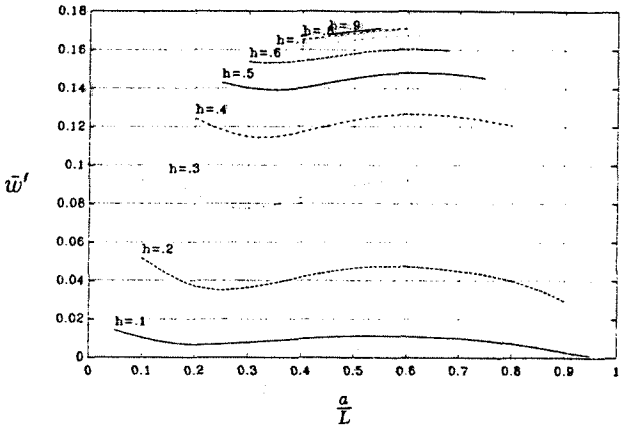

Figure 20: Mean square tip-section rotation of a cantilever beam (load frequency = 30 rad/s)

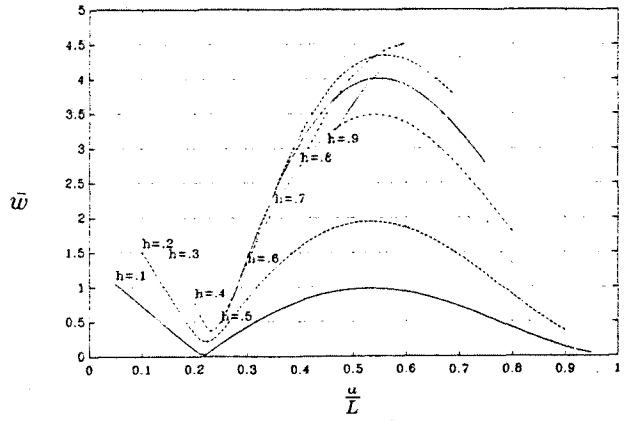

Figure 21: Mean square tip-deflection of a cantilever beam (load frequency = 64.7 rad/s)

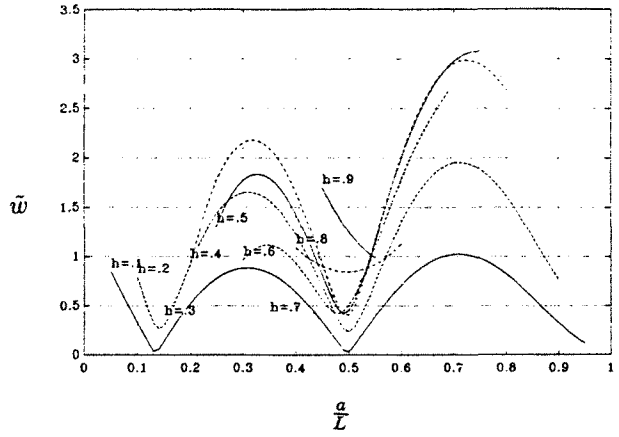

Figure 22: Mean square tip-deflection of a cantilever beam (load frequency = 181.3 rad/s)

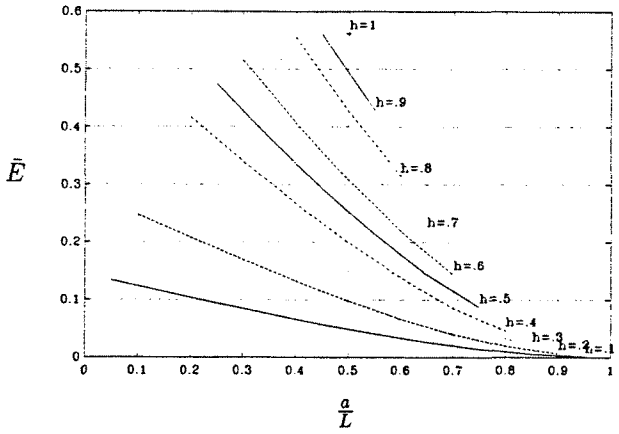

Figure 23: Mean square acoustic energy of a cantilever beam (load frequency = 10.3 rad/s)

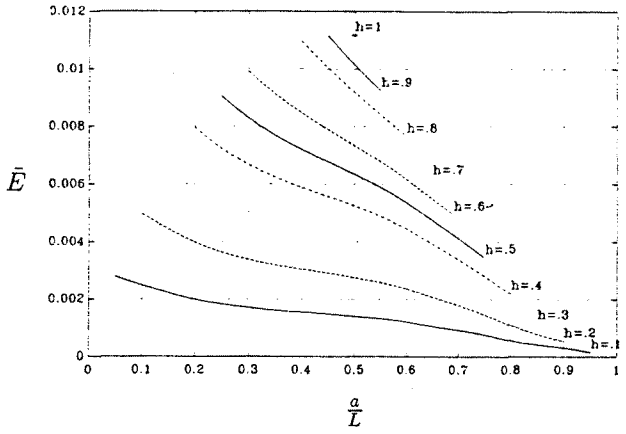

Figure 24: Mean square acoustic energy of a cantilever beam (load frequency = 30 rad/s)

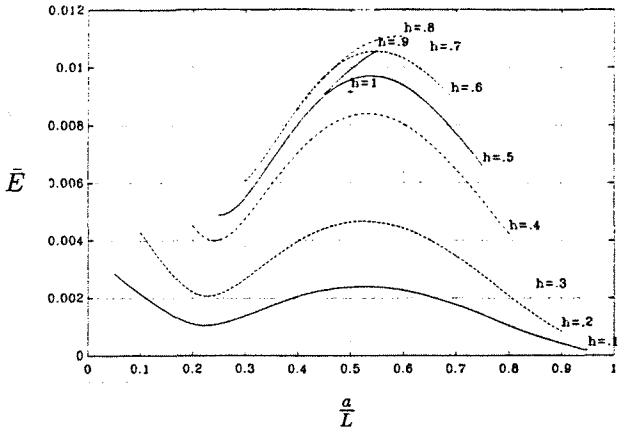

Figure 25: Mean square acoustic energy of a cantilever beam (load frequency = 50 rad/s)

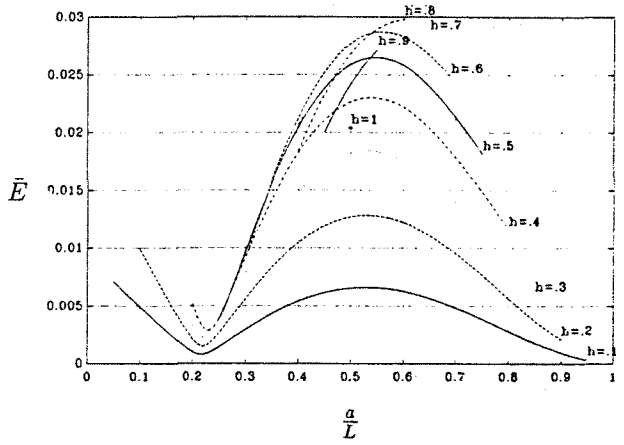

Figure 26: Mean square acoustic energy of a cantilever beam (load frequency = 70 rad/s)

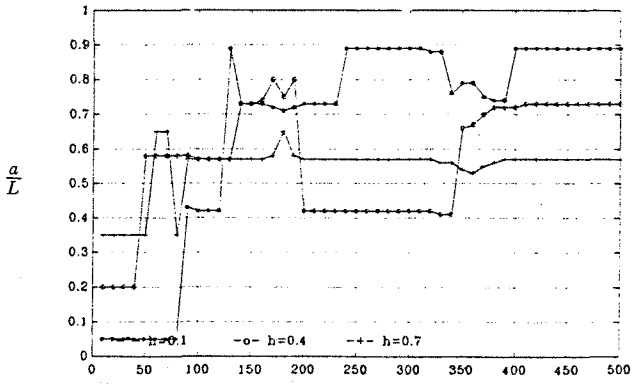

Figure 27: PZT optimal placement in a cantilever beam to perform high tip-deflection

($* \; h = 0.1$ $o \; h = 0.4$ $+ \; h = 0.7$)

Appendix

Dimensionless eigenmodes

In the following of the paper the $i-th$ natural spatial frequency $k_i = \sqrt{\sigma_i}$ is considered.

-Simply supported beam

$$X_i(\eta) = \sqrt{L}A_i \sin k_i\eta \tag{33}$$

$$\frac{\partial X_i}{\partial \eta} = \sqrt{L}A_i k_i \cos k_i\eta \tag{34}$$

$$\frac{\partial^2 X_i}{\partial \eta^2} = -\sqrt{L}A_i k_i^2 \sin k_i\eta \tag{35}$$

where

$$A_i = \sqrt{\frac{2}{L}} \qquad k_n = n\pi \tag{36}$$

-Cantilever beam

$$X_i(\eta) = \sqrt{L}A_i \cdot (\sin k_i\eta - c\cos k_i\eta - \sinh k_i\eta + c\cdot\cosh k_i\eta) \tag{37}$$

$$\frac{\partial X_i}{\partial \eta} = \sqrt{L}A_i k_i \cdot (\cos k_i\eta + c\cdot\sin k_i\eta - \cosh k_i\eta + c\cdot\sinh k_i\eta) \tag{38}$$

$$\frac{\partial^2 X_i}{\partial \eta^2} = \sqrt{L}A_i k_i^2 \cdot (-\sin k_i\eta + c\cdot\cos k_i\eta - \sinh k_i\eta + c\cdot\cosh k_i\eta) \tag{39}$$

where

$$A_i = \left(c^2 L + \frac{\sin 2k_iL}{4k_i}(c^2-1) - \frac{c}{k_i}\sin^2 k_iL - \frac{\sinh 2k_iL}{4k_i}(c^2-1) + \frac{1-c^2}{k_i}\cos k_iL\sinh k_iL - \frac{c^2+1}{k_i}\sin k_iL\cosh k_iL - \frac{c}{2k_i}(\cosh 2k_i - 1)\right)^{-\frac{1}{2}} \tag{40}$$

$$c = \frac{\sin k_i + \sinh k_i}{\cos k_i + \cosh k_i} \tag{41}$$

-Clamped beam

$$X_i(\eta) = \sqrt{L}A_i(\sin k_i\eta - c\cdot\cos k_i\eta - \sinh k_i\eta + c\cdot\cosh k_i\eta) \tag{42}$$

$$\frac{\partial X_i}{\partial \eta} = \sqrt{L}A_i k_i(\cos k_i\eta + c\sin k_i\eta - \cosh k_i\eta + c\cdot\sinh k_i\eta) \tag{43}$$

$$\frac{\partial^2 X_i}{\partial \eta^2} = \sqrt{L}A_i k_i^2(-\sin k_i\eta + c\cos k_i\eta - \sinh k_i\eta + c\cdot\cosh k_i\eta) \tag{44}$$

where

$$A_i = \left(c^2 L + (1+c^2)\frac{\sinh 2k_iL}{4k_i} + (-1)^n(1+c^2)\frac{\cosh k_iL}{k_i} + 2(-1)^{n+1}\frac{c}{k_i}\sinh k_iL + \frac{c}{2k_i}(1-\cosh 2k_iL)\right)^{-\frac{1}{2}} \tag{45}$$

$$c = \frac{\sin k_i - \sinh k_i}{\cos k_i - \cosh k_i} \tag{46}$$

-Supported-clamped beam

$$X_i(\eta) = \sqrt{L}A_i \cdot (\sin k_i\eta - c\cdot\sinh k_i\eta) \tag{47}$$

$$\frac{\partial X_i}{\partial \eta} = \sqrt{L}A_i k_i \cdot (\cos k_i\eta - c\cdot\cosh k_i\eta) \tag{48}$$

$$\frac{\partial^2 X_i}{\partial \eta^2} = \sqrt{L}A_i k_i^2 \cdot (-\sin k_i\eta - c\cdot\sinh k_i\eta) \tag{49}$$

where

$$A_i = \left(\frac{L}{2}(1-c^2) + \frac{(c^2\sinh 2k_iL - 1)}{4k_i} - (-1)^n\frac{\sqrt{2}c}{2k_i}e^{-k_iL}\right)^{-\frac{1}{2}} \tag{50}$$

$$c = \frac{\sin k_i}{\sinh k_i} \tag{51}$$

The following is a list of the first six eigenfrequencies of the cantilever beam considered:

Eigenfrequencies (rad/s)					
ω_1	ω_2	ω_3	ω_4	ω_5	ω_6
10.34	64.77	181.37	355.41	587.53	877.67

References

1. Rogers C.A.,"Intelligent Material Systems - The Dawn of a New Materials Age",*Journal of Intelligent Material Systems and Structures*, 1982, Vol.4, No. 1, pp. 742-754.

2. Wada B., Fanson J.L., Crawley E.F., "Adaptive Structures", in B.Wada editor, Adaptive Structures, (1-8), New York, 1989, ASME.

3. "IEEE Standard on Piezoelectricity", 1978.New York: The Institute of Electrical Electronics Engineers.

4. Crawley E.F., de Luis J., "Use of Piezoelectric Actuators as Elements of Intelligent Structures", *AIAA Journal*, 1987, Vol. 25 (10), pp. 1373-1385.

5. Barboni R. Gaudenzi P. Strambi G. "On the Stress Distribution in a Simple Adaptive Structure Actuated in Bending Mode", Second European Conference on Smart Structure and Materials, Glasgow 1994, SPIE volume 2361,pp.71-74.

6. Cauldhry Z., Rogers C.A., "The Pin-Force Model Revisited", *Journal of Intelligent Material Systems and Structures*, 1994, Vol.5,pp.347-353.

7. Strambi G., Barboni R. , Gaudenzi P. "Pin-Force and Euler-Bernoulli Models for Analysis of Intelligent Structures.",*AIAA Journal*, Vol.33 n.9, pp. 1746-1749.

8. Dimitriadis E.K., Fuller C.R., Rogers C.A., "Piezoelectric Actuators for Distributed Vibration Excitation of Thin Plates", *Journal of Vibration and Acoustics*, 1989,113, pp.100-107.

9. Tzou H.S.,Tseng C.I.,"Distributed Vibration Control and Identification of Coupled Elastic/ Piezoelectric Systems: Finite Element Formulation and Applications", *Mechanical Systems and Signal Processing*,1991,Vol.5.pp.215-231.

10. Ha S.K., Keilers C., Chang K.K., "Analysis of Laminated Composites Containing Distributed Piezoelectric Ceramics", *Journal of Intelligent Material Systems and Structures*, 1991, Vol. 2, pp. 59-71.

11. Gaudenzi P.,Bathe K.J.,"An Iterative Finite Element Crocedure for the Analysis of Piezoelectric aontinua",*Journal of Intelligent Material Systems and Structures*,1995, Vol.6,pp.266-273.

12. Hagood N.W.,Von Flotow A.,"Damping of Structural Vibrations with Piezoelectric Materials and Passive Electrical Networks", *Journal of Sound and Vibration*,1991, 146,pp.243-268.

13. Wang, B.-T., Rogers C.A. "Modeling of Finite-Length Spatially-Distributed Induced Strain Actuators for Laminate Beams and Plates." *Journal of Intelligent Material Systems and Structures* 1991, Vol. 2, pp.38-58.

14. Lin Y.H., Chu L., "Numerical Evaluation for Stability and Performance of an Electronic Damping Device for Structural Vibration Control", *Journal of Sound and Vibration* , 1994, 184, 929-933.

15. D'Cruz J.,"Global Multivariable Vibration Control with Distributed Piezoceramic Actuators",*Journal of Intelligent Material Systems and structures* ,1995, Vol.6,pp.419-429.

16. Lai Z.,Xue D.Y.,Huang J.K.,Mei C.,"Panel flutter Limit-Cycle Suppression with Piezoelectric Actuation", *Journal of Intelligent Material Systems and Structures*,1995, Vol.6,pp.274-281.

17. Hagood W., Chung W., Von Flotow A., "Modelling of Piezoelectric Actuator Dynamics for Active Structural Control", *Journal of Intelligent Material Systems and Structures*, 1990,Vol.1,pp.327-354.

18. Lester H.,Lefebvre S.,"Piezoelectric Actuator Models for Active Sound and Vibration Control of Cylinders", *Journal of Intelligent Material Systems and Structures*,1993,Vol.4,pp.295-306.

19. Ko B.,Tongue B.H.,"Acoustic Control using a Self-Sensing Actuator",*Journal of Sound and Vibration*,1994,187,pp.145-165.

20. Dosch J., Inman D.,Garcia E., "A Self-Sensing Piezoelectric Actuator for Collocated Control", *Journal of Intelligent Material Systems and structures*, 1992, Vol.3,pp.166-185.

21. Lee C.K., Moon F.C. , "Modal Sensors/ Actuators", *Transaction of the ASME*, 1990, Vol. 7, pp. 434-441.